

## Transport near the metal-insulator transition: Polypyrrole doped with PF<sub>6</sub>

C. O. Yoon, Reghu M., D. Moses, and A. J. Heeger

*Institute for Polymers and Organic Solids, University of California at Santa Barbara, Santa Barbara, California 93106*

(Received 30 November 1993)

Heavily doped polypyrrole-hexafluorophosphate, PPy(PF<sub>6</sub>), undergoes a metal-insulator (*M-I*) transition at resistivity ratio  $\rho_r = \rho(1.4 \text{ K})/\rho(300 \text{ K}) \approx 10$ : for  $\rho_r < 10$ , the system is metallic with  $\rho(T)$  remaining finite as  $T \rightarrow 0$ , whereas for  $\rho_r > 10$ , the system is an insulator with  $\rho \rightarrow \infty$  as  $T \rightarrow 0$ . In the critical regime,  $\rho(T)$  shows a power-law temperature dependence,  $\rho(T) = T^{-\beta}$ , with  $0.3 < \beta < 1$ . The effect of the partially screened Coulomb interaction is substantial at low temperatures for samples on both sides of the *M-I* transition. In the insulating regime, the crossover from Mott variable-range hopping (VRH) to Efros-Shklovskii hopping is observed. In the metallic regime, the sign of the temperature coefficient of the resistivity changes at  $\rho_r \approx 2$ . At  $T = 1.4 \text{ K}$ , the interaction length  $L_T = (\hbar D/k_B T)^{1/2} \approx 30 \text{ \AA}$ . Since this is smaller than the inelastic-scattering length,  $L_{in} \approx 300 \text{ \AA}$ , the contribution to  $\rho(T)$  from the electron-electron interaction is dominant. Application of high pressure decreases  $\rho_r$ , induces the transition into the metallic regime, and enables fine tuning of the *M-I* transition. For samples close to the *M-I* transition, the thermoelectric power is proportional to the temperature in both the metallic and insulating regimes. The correlation length ( $L_c$ ) increases as the disorder, characterized by  $\rho_r$ , approaches the *M-I* transition from either side. The expected divergence in  $L_c$  at the *M-I* transition is qualitatively consistent with the values for  $L_c$  inferred from the extrapolated  $\sigma(0)$  in the metallic regime and from analysis of the VRH magnetoresistance in the insulating regime. Thus, by using  $\rho_r$  to characterize the magnitude of the disorder, a complete and fully consistent picture of the *M-I* transition in PPy(PF<sub>6</sub>) is developed.

### I. INTRODUCTION

Recent studies of doped polypyrrole (PPy), polymerized electrochemically at relatively low temperatures ( $-20^\circ\text{C}$  to  $-30^\circ\text{C}$ ), have shown that the room-temperature conductivity  $\sigma_{RT} \approx 200\text{--}500 \text{ S/cm}$ , increasing to approximately  $1000 \text{ S/cm}$  after tensile drawing.<sup>1-3</sup> A positive temperature coefficient of the resistivity (TCR) was reported for temperatures below  $T = 10\text{--}20 \text{ K}$  for PF<sub>6</sub>-doped PPy, PPy(PF<sub>6</sub>).<sup>2,3</sup> To date, however, the physical aspects of these phenomena as related to the metallic nature of heavily doped conjugated polymers have not been clearly understood. Models suggested earlier,<sup>2,3</sup> such as the electron-hopping (or tunneling) conduction, small-polaron tunneling,<sup>4</sup> local superconductivity,<sup>2</sup> etc. seem to be either inappropriate or incapable of describing the entire range for the data (i.e., in both metallic and insulating samples).<sup>5</sup>

Many of the properties that characterize heavily doped conducting polymers, such as relatively high electrical conductivity,<sup>6-8</sup> temperature independent magnetic susceptibility,<sup>9</sup> linear temperature dependence of thermoelectric power,<sup>10,11</sup> absorption throughout the infrared with no energy gap,<sup>12</sup> etc., suggest that the electronic structure is that of a metal. However, the disorder generated during synthesis and during the doping process plays a critical role; microscopic disorder and/or structurally amorphous regions can dominate the transport.

We present the results of a systematic study of the transport properties of PPy(PF<sub>6</sub>) near the disorder-induced metal-to-insulator (*M-I*) transition. The extent

of disorder was characterized by the magnitude of the resistivity ratio,  $\rho_r = \rho(1.4 \text{ K})/\rho(300 \text{ K})$ . The *M-I* transition occurs at  $\rho_r \sim 10$ . In the metallic regime, the sign of the temperature coefficient of the resistivity changes at low temperatures due to the electron-electron interaction. In the insulating regime, the crossover from Mott variable-range hopping conduction<sup>13</sup> to Efros-Shklovskii hopping conduction<sup>14</sup> is observed, again as a result of the Coulomb interaction. Pressure increases the interchain coupling and decreases  $\rho_r$ , thereby inducing the transition from insulator to metal and enabling fine tuning of the *M-I* transition. The magnetoresistance is positive and large at low temperatures. The thermoelectric power shows a linear temperature dependence in both the metallic and the insulating regimes.

### II. EXPERIMENTAL DETAILS

PPy(PF<sub>6</sub>) films were prepared by anodic oxidation of pyrrole in an electrochemical cell containing 0.06M of pyrrole monomer, 0.06M of tetrabutylammonium hexafluorophosphate and 1 volume % of water in propylene carbonate (PC) under nitrogen atmosphere.<sup>1-2</sup> A glassy carbon electrode and platinum foil were used for the working and counter electrodes, respectively. A constant current ( $0.1\text{--}0.3 \text{ mA/cm}^2$ ) was applied, and the polymerization temperature was maintained at either  $-40^\circ\text{C}$  or at room temperature. Free-standing films with thicknesses from 5 to 15  $\mu\text{m}$  were peeled off the electrode, washed in pure PC, and dried under vacuum for 24 h at room temperature.

The four terminal technique was used for the dc con-

ductivity measurements. Electrical contacts were made with conducting graphite adhesive. High-pressure conductivity measurements were carried out using self-clamped beryllium-copper pressure cells.<sup>15</sup> After pressurization, the cell was clamped at room temperature and then cooled down to 1.3 K in a cryostat containing a superconducting magnet (0–10 T). The hydrostatic pressure transmitting medium was fluorinert. Temperature was measured with a calibrated platinum resistor (300 K–40 K) or a calibrated carbon glass resistor (40–1.3 K) and varied with a temperature controller driven by the computer. Magnetoresistance measurements were carried out with the current direction parallel to the magnetic field.

The differential technique<sup>16</sup> was used for the thermoelectric power measurements. Two isolated copper blocks were alternatively heated with the heating current accurately controlled by the computer. The temperature difference between the two copper blocks was measured by a chromel-constantan thermocouple. Samples were mounted across the copper blocks with pressure contacts, and the voltage difference across the sample was averaged for one complete cycle. The thermometry was calibrated for the entire temperature range ( $5 < T < 300$  K). The absolute thermoelectric power of the sample was obtained using the absolute scale for lead.<sup>17</sup>

### III. RESULTS AND DISCUSSION

#### A. Temperature dependence of the resistivity

Figure 1 shows the temperature dependence of resistivity normalized by  $\rho(300\text{ K})$  for samples prepared under different polymerization conditions. Throughout the following discussion, samples are denoted as follows: *M* indicates the metallic regime; *Mc* indicates the metallic regime but close to the *M-I* transition; *c* indicates the critical regime; *Ic* indicates the insulating regime but close to the *M-I* transition; and *I* indicates the insulating regime.

The room temperature conductivity for the films grown at  $-40^\circ\text{C}$  is typically  $\sigma(300\text{ K}) \sim 100\text{--}400\text{ S/cm}$  (e.g., samples *M*, *Mc*, and *Ic*). The temperature dependence of the resistivity is sensitive to the polymerization conditions. Films prepared at room temperature (samples *I*) show  $\sigma(300\text{ K}) \approx 20\text{--}50\text{ S/cm}$  and exhibit a strong temperature dependence of the resistivity at low tempera-

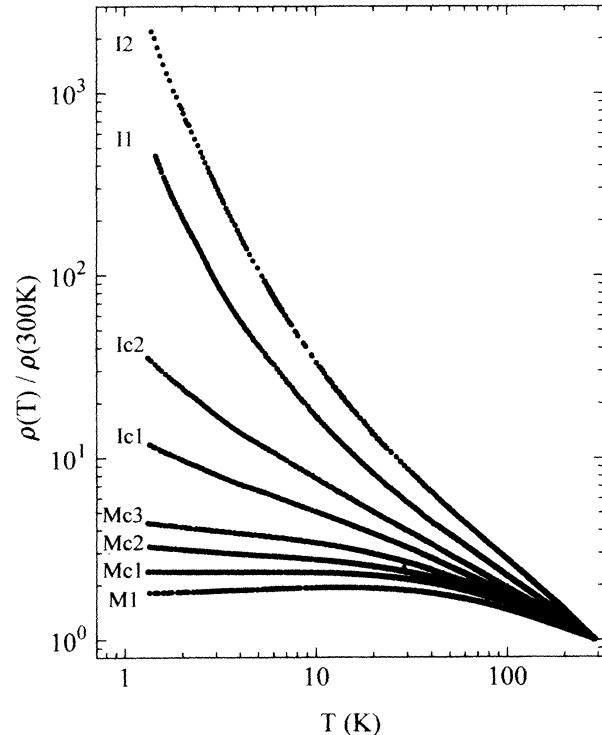


FIG. 1. Log-log plots of the temperature dependence of the resistivity,  $\rho(T)$ , of PPy-PF<sub>6</sub>. The resistivities are normalized by  $\rho(300\text{ K})$ . The values for  $\sigma(300\text{ K})$  and  $\rho_r = \rho(1.4\text{ K})/\rho(300\text{ K})$  are listed in Tables I and II.

ture. For samples with higher conductivity,  $\sigma(300\text{ K}) > 200\text{ S/cm}$  (samples *M*), the resistivity at low temperatures decreases as the temperature is lowered showing a resistivity maximum around  $T \sim 7\text{--}20\text{ K}$ . The results and the various parameters obtained from the data are listed in Tables I and II.

We characterize the transport properties of the PF<sub>6</sub>-doped polypyrrole in terms of the resistivity ratio,  $\rho_r = \rho(1.4\text{ K})/\rho(300\text{ K})$ . (i) Insulating regime ( $\rho_r > 100$ ): the resistivity is strongly activated (sample *I*); (ii) insulating side of the *M-I* transition ( $10 < \rho_r < 100$ ): the resistivity has a power-law temperature dependence for  $T > 30\text{ K}$ , and  $\rho(T)$  is weakly activated at low temperatures (sample *Ic*); (iii) metallic side of the *M-I* transition ( $2 < \rho_r < 6$ ): zero-temperature limit of the conductivity

TABLE I. Experimental values and parameters for samples in the insulating regime.

Sample	$\sigma(300\text{ K})$ (S/cm)	$\rho_r^a$	$\Delta\rho/\rho^b$	$x^c$	$T_{\text{Mott}}^d$ (K)	$L_c$ (Å)
<i>Ic1</i>	114	11.6	0.40	$0.19 \pm 0.03$ ( $T < 4\text{ K}$ )	20	269
<i>Ic2</i>	103	35.8	0.51	$0.24 \pm 0.02$ ( $T < 5\text{ K}$ )	290	177
<i>I1</i>	52	527		$0.24 \pm 0.02$ ( $T > 5\text{ K}$ )	3 700	
<i>I2</i>	34.4	2590	1.78	$0.29 \pm 0.03$ ( $T > 2\text{ K}$ )	17 500	86

<sup>a</sup> $\rho_r = \rho(1.4\text{ K})/\rho(300\text{ K})$ .

<sup>b</sup>Data at  $H = 8\text{ T}$  and at  $T = 1.4\text{ K}$ .

<sup>c</sup>Results from data using Eq. (4).

<sup>d</sup>Values are obtained assuming  $x = 0.25$ .

TABLE II. Experimental values and parameters for samples in the metallic regime.

Sample	Pressure	$\sigma(300\text{ K})$ (S/cm)	$\rho_r^a$	$\Delta\rho/\rho^b$	$m^c$	$m'^c$	$\sigma(0)^d$ (S/cm)	$L_c^e$ (Å)	$T_m$ (K)
<i>M1</i>	ambient	338	1.75	0.12	-7.55	+7.80	201	12.1	12
<i>M2</i>	ambient	298	1.97	0.13	-3.19	+8.34	155	15.7	7.5
<i>M2</i>	9 kbar	330	1.33	0.05	-8.83	+0.86	261	9.3	24
<i>Mc1</i>	ambient	271	2.40	0.16	+1.75	+11.6	108	22.5	
<i>Mc2</i>	ambient	313	3.22	0.21	+12.9	+25.9	82	29.4	
<i>Mc2</i>	4 kbar	358	1.81	0.12	-3.98	+10.2	191	12.7	12
<i>Mc2</i>	10 kbar	377	1.54	0.10	-9.13	+6.22	247	9.8	19
<i>Mc3</i>	ambient	192	4.45	0.23	+8.00	+12.9	34	70.9	
<i>Ic1</i>	4 kbar	133	2.64	0.18	+2.05	+6.83	46	52.6	
<i>Ic1</i>	10 kbar	137	2.08	0.15	-0.20	+5.11	64	37.8	

<sup>a</sup> $\rho_r = \rho(1.4\text{ K})/\rho(300\text{ K})$ .

<sup>b</sup>Data at  $H=8\text{ T}$  and at  $T=1.4\text{ K}$ .

<sup>c</sup>In units of  $\text{S/cm K}^{1/2}$ .

<sup>d</sup>Extrapolated values from square-root  $T$  dependence of the conductivity.

<sup>e</sup>Calculated from the relation  $\sigma(0)=0.1e^2/\hbar L_c$ .

$\sigma(0)$ , is finite, but the TCR remains negative (samples *Mc*); (iv) metallic regime ( $\rho_r < 2$ ): TCR is positive at low temperatures with a conductivity minimum at  $T=T_m$  (sample *M*). The existence of finite conductivity extrapolated to  $T=0\text{ K}$ ,  $\sigma(0)$ , is considered as defining the boundary of the *M-I* transition; for PPy(PF<sub>6</sub>), this occurs at  $\rho_r \approx 10$ . The sign of the TCR changes on the metallic side of *M-I* transition, at  $\rho_r \approx 2$ .

To explicitly describe the characteristic behavior of  $\rho(T)$ , we define the reduced activation energy as the logarithmic derivative of  $\rho(T)$ ,<sup>18</sup>

$$W = -T \{ d \log_{10} \rho(T) / dT \} = -d(\log_{10} \rho) / d(\log_{10} T). \quad (1)$$

The plots of  $\log_{10} W$  vs  $\log_{10} T$  shown in Fig. 2 have “tree-like” structure with “metallic” ( $dW/dT < 0$ ) and “insulating” ( $dW/dT > 0$ ) branches at low temperature.<sup>18</sup>

The power-law dependence of  $\rho(T)$  is characteristic of the critical regime of the *M-I* transition. For the temperature region showing power-law dependence,  $\rho(T) \propto T^{-\beta}$ , the exponent  $\beta$  can be determined from Eq. (1),

$$W = \beta, \quad (2)$$

where  $\beta$  varies from 0.3 to 1 as  $\rho_r$  increases across the critical regime from the metal (smallest  $\beta$ ) to the insulator (largest  $\beta$ ) side.

For insulating samples (*I* and *Ic*), the low-temperature resistivity follows the exponential temperature dependence characteristic of variable-range hopping (VRH),

$$\rho(T) = \rho(0) \exp\{-(T_0/T)^x\}, \quad (3)$$

where  $x = \frac{1}{4}$  for three-dimensional hopping of noninteracting carriers,<sup>13</sup> and  $x = \frac{1}{2}$  in the Efros-Shklovskii (ES) limit<sup>14</sup> where the Coulomb interaction between the electron and the hole left behind is the dominant energy; i.e., when there is a Coulomb gap in the density of states near the Fermi level.<sup>14</sup> From Eq. (1), the reduced activation energy becomes

$$\log_{10} W(T) = A - x \log_{10} T, \quad (4)$$

where  $A = x \log_{10} T_0 + \log_{10} x$ . Using Eq. (4), one can determine both  $T_0$  and  $x$  from the data (see Table I). The barely insulating samples (*Ic*) show VRH temperature dependence with  $x = \frac{1}{4}$  below  $T \approx 5\text{ K}$ . A crossover from Mott ( $x = \frac{1}{4}$ ) to ES ( $x = \frac{1}{2}$ ) VRH temperature dependence is observed for samples *I1* and *I2*, which are farther into the insulating regime with larger  $\rho_r$ , at  $T=5\text{ K}$  and  $2\text{ K}$ , respectively (see data for sample *I1* in the inset of Fig. 2). For samples in the metallic regime (*Mc*, *M*),  $W(T)$  remains small at low temperature. The curious minimum of  $W(T)$  at  $T \approx 3-5\text{ K}$  for barely metallic samples

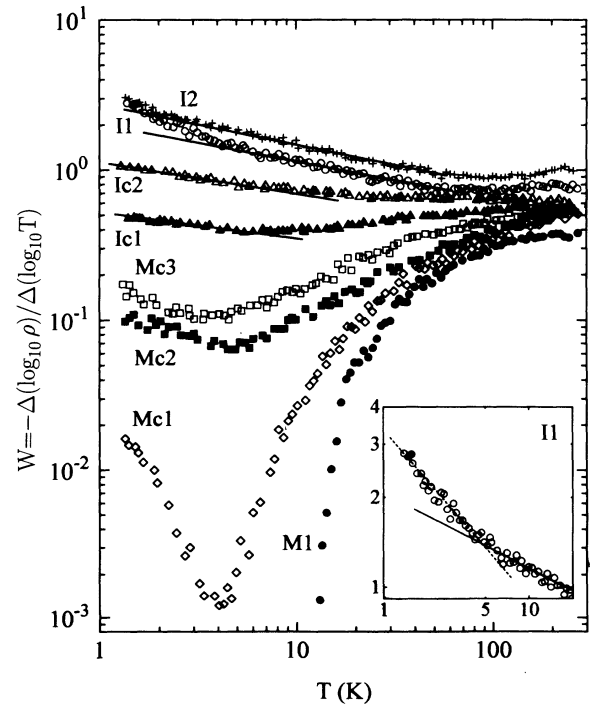


FIG. 2.  $W = -(\Delta \log_{10} \rho / \Delta \log_{10} T)$  vs  $T$  (log-log plot) for various PPy(PF<sub>6</sub>) samples. The inset shows data for sample *I1* for  $T < 20\text{ K}$ .

( $Mc, 2 < \rho_r < 6$ ) is a precursor of the change in the dominant transport mechanism at low temperatures; for metallic samples ( $M, \rho_r < 2$ ), the sign of  $W(T)$  remains negative below  $T_m \approx 7-25$  K.

For a three-dimensional system close to the  $M-I$  transition, the correlation length ( $L_c$ ) is large and has a power-law dependence on  $\delta = |E_F - E_c|/E_F \ll 1$  with critical exponent  $\nu$ ,  $L_c = a\delta^{-1/\nu}$ , where  $a$  is a microscopic length,  $E_F$  is the Fermi energy, and  $E_c$  is the mobility edge.<sup>19</sup> In this critical region, the resistivity is not activated, but follows a power law as a function of temperature.<sup>20</sup> As shown by Larkin and Khmel'nitskii,<sup>21</sup>

$$\rho(T) = (e^2 p_F / \hbar^2) (k_B T / E_F)^{-1/\eta} \propto T^{-\beta}, \quad (5)$$

where  $p_F$  is the Fermi momentum,  $e$  is the electron charge, and  $1 < \eta < 3$ . The latter is consistent with the observed values for  $\beta$ ,  $0.3 < \beta = 1/\eta < 1$ . According to McMillan's scaling theory,<sup>20</sup> the energy scale of the system (the correlation gap) in the crossover from the critical regime to the metallic or insulating regime is  $\Delta_c = (\hbar D_a / a^2) (a / L_c)^\eta$ , where  $D_a$  is the diffusion constant on the microscopic length scale. The correlation gap is related to the characteristic crossover temperature ( $T_{\text{corr}}$ ) from the power-law dependence of the resistivity at high temperatures to the exponential dependence of the resistivity at low temperatures (insulating regime) or to the square-root  $T$  dependence of the conductivity with finite  $\sigma(T \rightarrow 0)$  (metallic regime). The power-law dependence observed down to  $T_{\text{corr}} \approx 10$  K for the barely insulating sample ( $Ic$ ) corresponds to the critical divergence of  $L_c$  very close to the  $M-I$  transition.

The partial screening of the Coulomb interaction plays an important role at low temperature with a square-root singularity in the one-electron density of states at the Fermi level,<sup>14,22</sup> in both conducting and insulating phases. The observation of the crossover from Mott to Efros-Shklovskii VRH conduction in the insulating regime is an indication of the importance of the long-range Coulomb interaction. In the metallic regime, the conduction mechanism at low temperature ( $T < T_{\text{corr}}$ ) is via quantum diffusion of quasiparticles, and the conductivity at finite temperature can be expressed as,

$$\begin{aligned} \sigma(T) &= \sigma(0) + \Delta\sigma_I(T) + \Delta\sigma_L(T) \\ &= \sigma(0) + mT^{1/2} + BT^{p/2}, \end{aligned} \quad (6)$$

where  $\sigma(0) \sim 0.1e^2/\hbar L_c$ ,<sup>20</sup> the second term is the lowest-order correction to the conductivity arising from electron-electron interactions,<sup>22,23</sup> and the last term is the finite temperature localization correction in the weakly disordered limit.<sup>24</sup> The temperature dependence of the localization correction is determined by the temperature dependence of the inelastic-scattering rate  $\tau_{\text{in}}^{-1} = T^p$  of the dominant dephasing mechanism. For electron-phonon scattering,  $p = 2.5-3$ ; for inelastic electron-electron scattering,  $p = 2$  and  $1.5$  in the clean and dirty limits, respectively.<sup>25</sup> The calculation by Belitz and Wysokinski<sup>26</sup> gives  $p = 1$  very near the  $M-I$  transition. The most important contribution to the conductivity depends on the size of three length scales:<sup>27,28</sup> the correlation length  $L_c$ ,

the interaction length  $L_T = (\hbar D / k_B T)^{1/2}$ , and the inelastic diffusion length  $L_{\text{in}} = (D \tau_{\text{in}})^{1/2}$ . In practice, however, it is difficult to distinguish these contributions only from the temperature dependence of the conductivity. Since the coefficient  $m$  in Eq. (6) can have either sign depending on the competition between the Hartree contribution and the exchange contribution, the observed positive TCR for samples in the metallic regime (sample  $M$ ,  $\rho_r < 2$ ) and negative TCR close to transition (samples  $Mc$  with  $2 < \rho_r < 6$ ) are thought to be associated with a breakdown of Thomas-Fermi screening near the  $M-I$  transition.<sup>29</sup> Detailed analysis of the effects of electron-electron interaction and the localization correction will be discussed later.

## B. Magnetoresistance

The magnetoresistance (MR) is positive for PPy(PF<sub>6</sub>), both in the insulating regime and in the metallic regime. Figure 3 shows  $\Delta\rho(H)/\rho(0)$  at  $T = 1.4$  K as a function of  $H^2$  for magnetic fields up to  $H = 8$  T. The large positive MR in the insulating regime,  $\Delta\rho/\rho(H = 8 \text{ T}) = 1.8$  (inset in Fig. 3.), is typically expected for variable-range hopping conduction.<sup>14</sup> The data are linear in  $H^2$  up to  $H = 3.5$  T. For samples near the  $M-I$  transition, a significant reduction in the MR is observed, and the linearity on  $H^2$  is limited to much lower fields ( $H < 2$  T). Negative magnetoresistance<sup>30</sup> due to quantum interference in the VRH regime was not observed in the PPy(PF<sub>6</sub>) system. In the metallic regime,  $\Delta\rho/\rho(H = 8 \text{ T}) = 0.05 \sim 0.2$  at  $T = 1.4$  K. We do not observe a crossover from positive to negative magnetoresistance. The negative contribution of MR expected in a weakly localized system<sup>31</sup> is evidently less than the positive contribution that arises from electron-electron interactions<sup>23</sup> in the metallic regime. We note that the MR can be another useful "measure" for doped PPy sample characteriza-

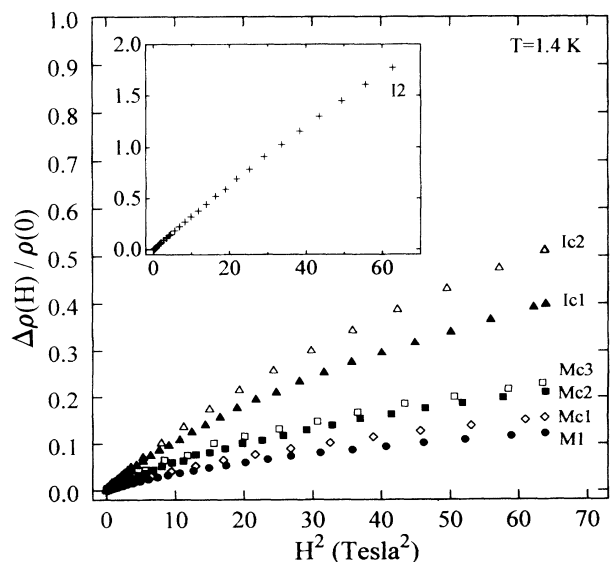


FIG. 3. The magnetoresistance of PPy(PF<sub>6</sub>) at  $T = 1.4$  K plotted as a function of  $H^2$  for  $H < 8$  T. The inset shows the magnetoresistance of an insulating sample.

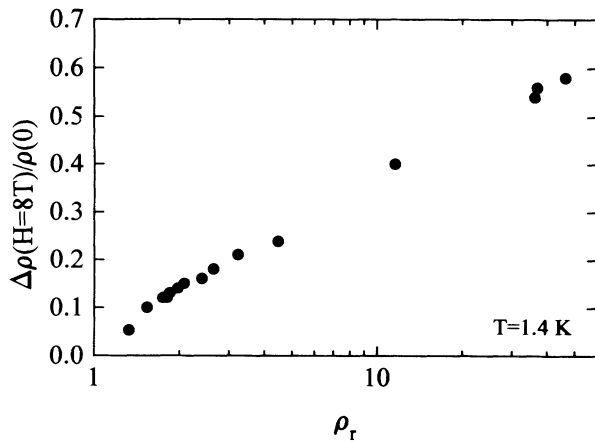


FIG. 4. The magnetoresistance of PPy(PF<sub>6</sub>) at  $H=8$  T and  $T=1.4$  K plotted as a function of  $\rho_r$ .

tion. Figure 4 shows a good correlation between  $\Delta\rho(H)/\rho(0)$  and  $\rho_r$ .

### C. Effects of pressure and magnetic fields: Fine tuning of the $M-I$ transition

The conductivity of PF<sub>6</sub>-doped PPy samples increases under high pressure ( $P$ ). Figure 5 shows the pressure dependence of the room-temperature conductivity for samples in the different regimes. For insulating samples, the conductivity increases monotonically for pressures up to 18 kbar, while for samples near the  $M-I$  transition  $\sigma(P)$  saturates at high pressure. In the metallic regime,  $\sigma(P)$  increases up to 7 kbar and slowly decreases at higher pressure. Similar results have been observed in other heavily doped conducting polymer systems.<sup>32</sup>

Figure 6 shows the temperature dependence of the conductivity for a barely insulating sample ( $Ic1$ ) under pressure. At ambient pressure ( $\rho_r=12$ ),  $\sigma(T)$  tends to zero as  $T \rightarrow 0$ . The finite zero-temperature conductivity at

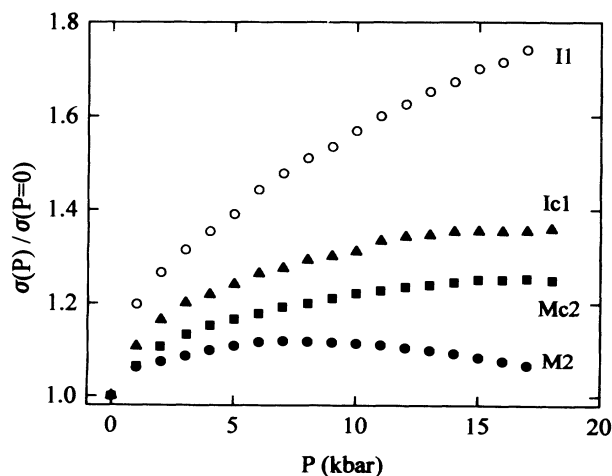


FIG. 5. Pressure dependence of the room-temperature conductivity; the data are normalized by the conductivity at ambient pressure.

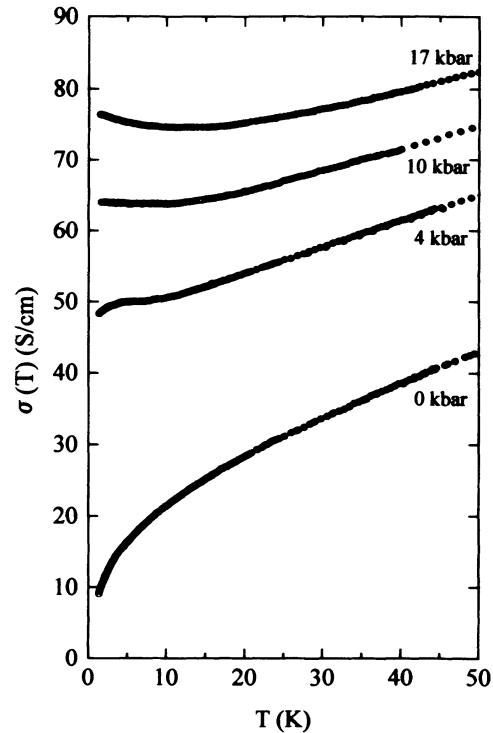


FIG. 6. Temperature dependence of the conductivity ( $T < 50$  K) of sample  $Ic1$  ( $\rho_r=12$ ) at different pressures.

$P=4$  kbar ( $\rho_r=2.64$ ) indicates that the  $M-I$  transition takes places between  $P=0$  and 4 kbar. The conductivity at  $P=10$  kbar ( $\rho_r=2.08$ ) is almost temperature independent. At still higher pressures ( $P=17$  kbar,  $\rho_r=1.83$ ), the low-temperature conductivity minimum is observed near  $T_m=13$  K. The plots of  $\log_{10}W(T)$  vs  $\log_{10}T$  as presented in Fig. 7 are remarkably similar to the data shown in Fig. 2. We find that all aspects of the pressure-induced  $M-I$  transition are directly analogous to the phenomena observed as a function of disorder at ambient pressure where  $\rho_r$  (which characterizes the disorder) is

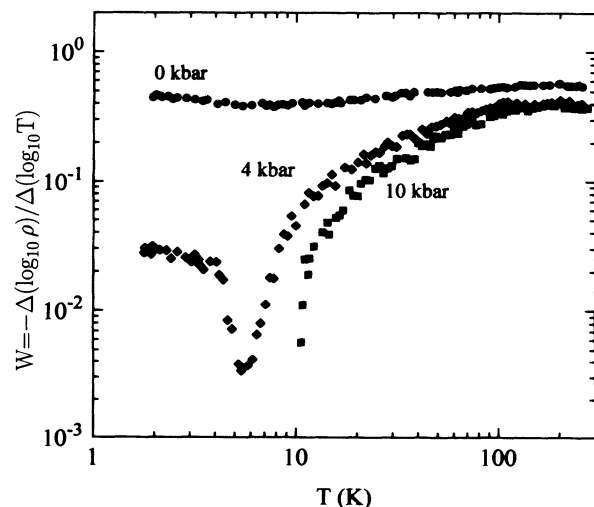


FIG. 7. Log-log plots of  $W = -(\Delta \log_{10} \rho / \Delta \log_{10} T)$  vs  $T$  for sample  $Ic1$  ( $\rho_r=12$ ) at different pressure.

the relevant variable.

The low-temperature conductivity anomaly in the metallic regime can be finely resolved through the pressure dependence of the conductivity for metallic samples [ $\sigma(T)$  finite as  $T \rightarrow 0$ ] near the critical regime (for example, *Mc2*). As shown in Fig. 8, pressures above 4 kbar decrease  $\rho_r$  from 3.22 to less than 2 and induce the positive TCR below  $T_m$  which increases from 12 K at  $P=4$  kbar to 21 K at 17 kbar. Free parameter fitting of the conductivity below 50 K to Eq. (6) gives  $p=2.50 \pm 0.04$  and  $B=0.40 \pm 0.01$ , independent of pressure (see the inset of Fig. 8). The exponent,  $p=2.5$ , of the localization correlation term in Eq. (6) implies that above  $T=T_m$  inelastic electron-phonon scattering is dominant.

The parameters  $\sigma(0)$  and  $m$  are pressure dependent; these parameters are also magnetic-field dependent, as shown in Fig. 9. As the temperature is lowered, the conductivity at  $H=8$  T begins to deviate from the zero-field data near  $T_m$ . At lower temperatures, the magnetic field decreases  $\sigma(0)$  and suppresses the positive TCR. As  $\rho_r$  decreases from 1.97 to 1.33,  $T_m$  increases from 7.5 to 24 K and the effect of an 8 T field becomes weaker. There exists a second temperature,  $T'_m$ , below which the conductivity at  $H=8$  T drops rapidly, indicative of the transition across the *M-I* boundary. The inset in Fig. 9 shows the inverse correlation between  $T_m$  and  $T'_m$ .

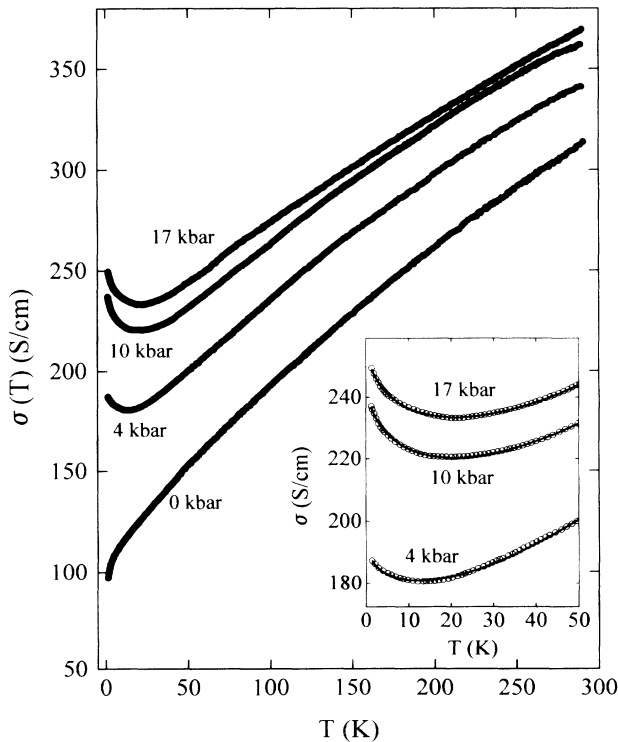


FIG. 8. The temperature dependence of the conductivity of *Mc2* ( $\rho_r=3.2$ ) at different pressure. The inset shows the same data below  $T=50$  K. Solid lines in the inset represent the fitted curve using  $\sigma(T)=\sigma(0)+mT^{1/2}+BT^{p/2}$ . The values of fitting parameters are given in the text.

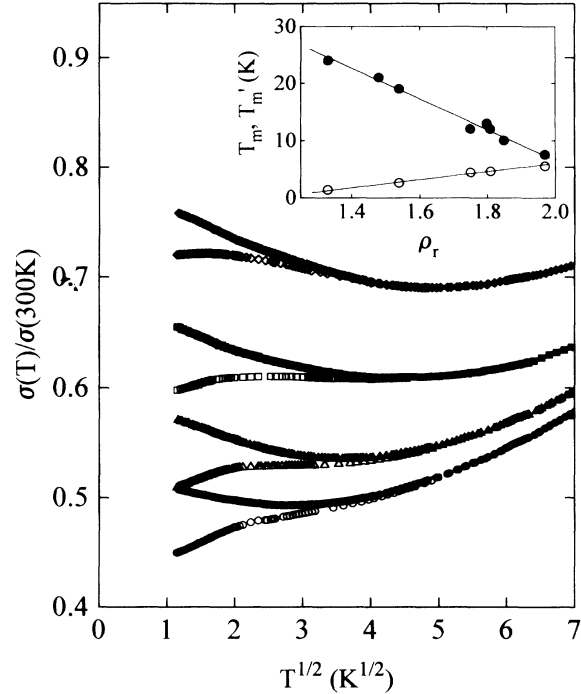


FIG. 9. Temperature dependence of the conductivity ( $T < 50$  K) normalized by  $\sigma(300$  K) for samples exhibiting positive TCR at low temperatures: (●) sample *M2* at  $P=9$  kbar ( $\rho_r=1.33$ ), (▲) sample *Mc2* at  $P=10$  kbar ( $\rho_r=1.54$ ), (■) sample *M1* at ambient pressure ( $\rho_r=1.75$ ), (◆) sample *M1* at ambient pressure ( $\rho_r=1.97$ ). Open symbols correspond to data at 8 T magnetic field. Data are plotted as a function of  $T^{1/2}$ . The inset shows  $T_m$  (●) and  $T'_m$  (○) as a function of  $\rho_r$ . The lines are drawn to guide eyes.

The crossover behavior of the TCR induced by pressure can be finely tuned by varying the magnetic field between  $0 < H < 8$  T. The data taken below  $T=4$  K, shown in Fig. 10, give straight lines vs  $T^{1/2}$ . In this temperature range, we ignore the last term in Eq. (6) and simply write

$$\sigma(T, H) = \sigma(0, H) + m(H)T^{1/2}. \quad (7)$$

The extrapolated values of  $\sigma(0, H \rightarrow 0) = \sigma(0, 0)$  and the field-dependent coefficients  $m = m(0)$ ,  $m' = m(H=8$  T) are listed in Table II.

Experimental values of  $\sigma(0)$  are well correlated with  $\rho_r$ ; however, values for the room-temperature conductivity show somewhat greater variation. We are able to get some insight into the sample and pressure dependence of the room-temperature conductivity for samples in the metallic regime,  $\sigma(300$  K) = 200–400 S/cm by plotting  $\sigma(0)$ ,  $\sigma(300$  K), and  $\rho_r\sigma(0)$  as a function of  $\rho_r$ ; see Fig. 11. As expected,  $\sigma(300$  K) and  $\rho_r\sigma(0)$  are approximately the same. The deviation between  $\sigma(300$  K) and  $\rho_r\sigma(0)$  for  $\rho_r > 3$  indicates a large temperature dependence between  $T=0$  and 1 K. The saturation of  $\sigma(300$  K) at  $\rho_r < 3$  is due to the increase in  $\sigma(0)$  and the decrease in  $\rho_r$ . The saturation, or the decrease of  $\sigma(300$  K) observed at high pressure (Fig. 5), has the same origin. Similar

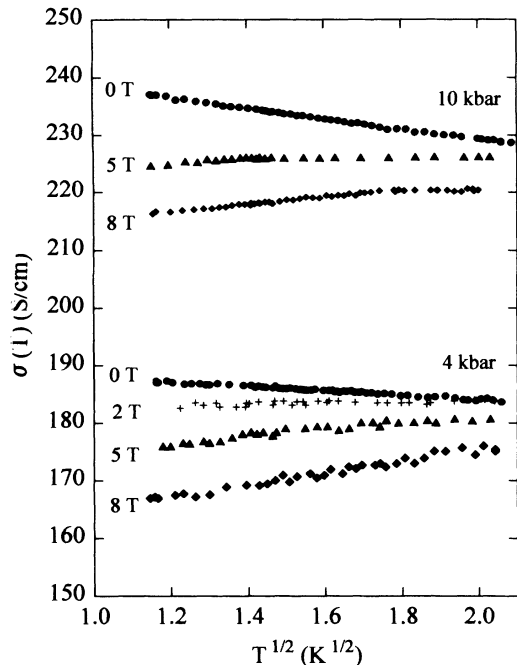


FIG. 10. Conductivity vs  $T^{1/2}$  at low temperature ( $1.3 \text{ K} < T < 4 \text{ K}$ ) for sample *Mc2* under  $P=4 \text{ kbar}$  ( $\rho_r=1.81$ ) and  $10 \text{ kbar}$  ( $\rho_r=1.54$ ) in various magnetic fields ( $H=0, 2, 5,$  and  $8 \text{ T}$ ).

behavior related to the decrease of conductivity at room temperature with weaker temperature dependence under pressure was observed in doped polyacetylene.<sup>32</sup>

#### D. The critical regime

The critical behavior of  $\sigma(0)$  predicted by the scaling theory of the  $M-I$  transition<sup>19</sup> is associated with correlation length  $L_c$  and disorder parameter  $k_F l$  ( $k_F$  is the Fermi momentum, and  $l$  is the mean free path). On the metallic side close to the  $M-I$  transition,

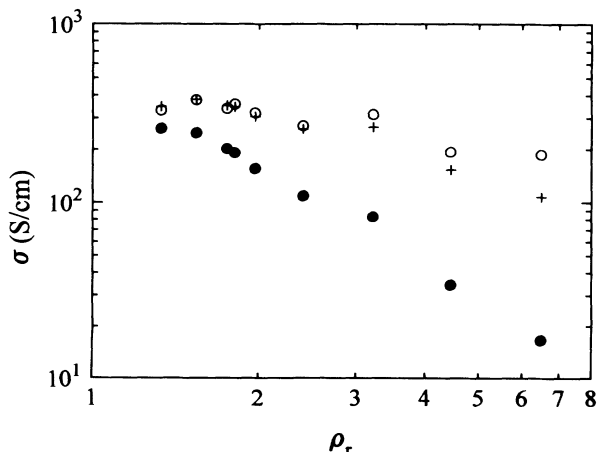


FIG. 11.  $\sigma(0)$  (●),  $\sigma(300 \text{ K})$  (○), and  $\rho_r \sigma(0)$  (+) plotted as a function of  $\rho_r$ .

$$\sigma(0) = \sigma_0(a/L_c) = \sigma_0(E_F - E_c/E_F)^{\nu}, \quad (8)$$

where  $\sigma_0$  depends on  $k_F l$ . When the mean free path is large ( $k_F l > 1$ ) the system is well into the metallic regime ( $E_F$  in a region of delocalized states far from  $E_c$ ),

$$\begin{aligned} \sigma(0) &= \sigma_0(e^2/\hbar)(n/k_F^2)(k_F l) \\ &= (e^2/\hbar)(1/3\pi^2)^{2/3} n^{1/3} k_F l, \end{aligned} \quad (9)$$

where  $n$  is the density of charge carriers. In the Ioffe-Regel limit,  $k_F l \sim 1$ ,  $\sigma_0 = e^2/3\hbar a$ ,<sup>13</sup> and  $\sigma(0)$  depends on  $L_c$ . Taking the carrier density for heavily doped PPy(PF<sub>6</sub>) as approximately  $n = 10^{21} \text{ cm}^{-3}$ ,<sup>33</sup> and  $\sigma(0) = 260 \text{ S/cm}$  for the most metallic sample, we obtain from Eq. (9)  $k_F l \approx 1.2$ , consistent with transport at the  $M-I$  boundary. The microscopic length scale of the system (a three-dimensional average of 4 pyrrole monomer unit cell spacing)  $a = n^{1/3} \approx 10 \text{ \AA}$  gives an estimate for Mott's minimum metallic conductivity<sup>13</sup> of  $\sigma_{\min} = 0.03e^2/\hbar a = 70 \text{ S/cm}$ , comparable in magnitude with the observed value (see Table II). Therefore, the critical behavior of  $\sigma(0)$  for PPy(PF<sub>6</sub>) is continuous, in agreement with the prediction of scaling theory, Eq. (8), including the effects of the electron-electron interaction and inelastic scattering.<sup>28</sup>

Pressure shifts the system toward the metallic regime and decreases  $\rho_r$ . As noted above, the trends are the same as those that result from disorder-induced variations of  $\rho_r$ . The significant difference of transport properties between films grown at  $-40^\circ\text{C}$  and films grown at room temperature implies that the decrease in disorder (resulting from lower temperature growth) is substantial. Since  $k_F l \approx 1.2$ , the critical behavior of  $L_c$  is important near the transition.

The mobility edge can be shifted by a magnetic field,<sup>34</sup> thereby decreasing  $\sigma(0)$ . In the metallic regime ( $E_F > E_c$ ), however, the correlation length is sufficiently smaller than magnetic length  $L_H = (c\hbar/eH)^{1/2}$  ( $= 90 \text{ \AA}$  at  $H = 8 \text{ T}$ ) that the correction to the conductivity resulting from an applied magnetic field is expected to be small. We find that the magnetoconductance is negative (magnetoconductance is positive), but large only at low temperatures ( $T < T_m$ ).

In this regime, the electron screening becomes less effective with the increasing disorder, and the contribution to the resistivity that arises from the long-range electron-electron interaction increases. According to the interaction theory,<sup>22,23</sup> the contribution of magnetoconductance due to electron-electron interaction is positive, and the sign of  $m$  changes as a function of disorder.

#### E. Effects of electron-electron interaction in the metallic regime

The finite temperature correction term in Eq. (7) calculated from the interaction theory<sup>23</sup> consists of exchange and Hartree contributions given by,

$$\Delta\sigma_I(T) = \alpha(4/3 - 3\gamma F_\sigma/2)T^{1/2} = mT^{1/2}, \quad (10a)$$

where

$$\alpha = (e^2/\hbar)(1.3/4\pi^2)(k_B/2\hbar D)^{1/2}, \quad (10b)$$

$$F_\sigma = 32\{(1+F/2)^{3/2} - (1+3F/4)\}/3F. \quad (10c)$$

The Hartree factor ( $F$ ) is the screened interaction averaged over the Fermi surface,  $D$  is the diffusion constant, and  $\gamma$  is a parameter that depends on the details of the scattering.<sup>35</sup> The sign of  $m$  is negative when the Hartree term in Eq. (10) dominates so that  $\gamma F_\sigma > \frac{8}{9}$ . In the presence of a magnetic field, the correction to the conductivity can be written as a sum of two terms,

$$\Delta\sigma_I(H, T) = \sigma_I(H, T) - \sigma_I(0, 0) = \Delta\sigma_I(T) + \Delta\Sigma_I(H, T). \quad (11)$$

The first term is the field independent exchange term and singlet Hartree contribution, and the second term is the triplet Hartree contribution. The magnetoconductance results from the second term in Eq. (11), with the following low-field and high-field limits:

$$\Delta\Sigma_I(H, T) = -0.41(g\mu_B/k_B)^2\gamma F_\sigma T^{-3/2}H^2, \quad g\mu_B/k_B T \ll 1 \quad (12a)$$

$$\Delta\Sigma_I(H, T) = \alpha g F_\sigma T^{1/2} - 0.77\alpha(g\mu_B/k_B)^{1/2}\gamma F_\sigma H^{1/2}, \quad g\mu_B/k_B T \gg 1, \quad (12b)$$

where  $g$  is the electron  $g$  value, and  $\mu_B$  is the Bohr magneton.

Figure 12(a) shows the magnetoconductance (at

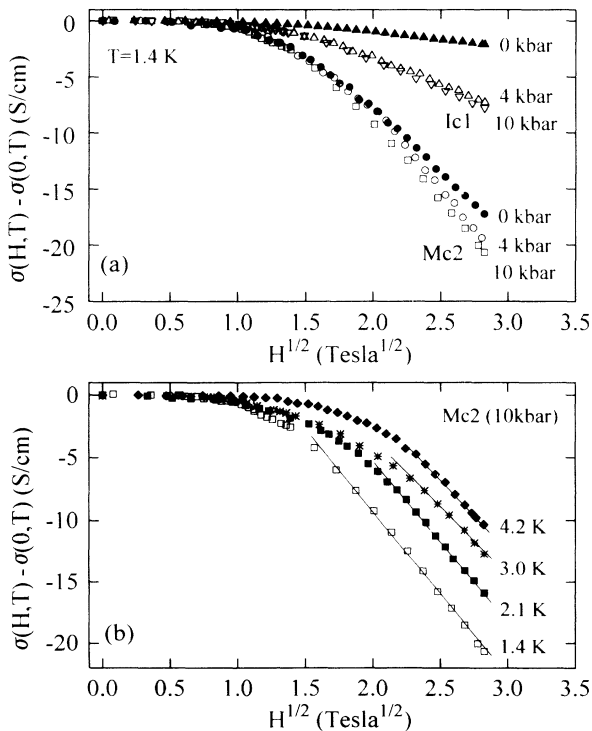


FIG. 12. High-field magnetoconductance of PPy(PF<sub>6</sub>) plotted as a function of  $H^{1/2}$ . (a) Magnetoconductance at  $T=1.4$  K for samples Ic1 and Mc2 at ambient pressure and at  $P=4$  and 10 kbar. (b) Magnetoconductance for sample Mc2 at 10 kbar, at various temperatures  $T=1.4, 2.1, 3.0,$  and  $4.2$  K.

$T=1.4$  K) of samples near the  $M-I$  transition, as a function of  $H^{1/2}$  up to  $H=8$  T. The magnetoconductance is negative and is proportional to  $H^{1/2}$  for  $H>4$  T. The slopes are more or less temperature independent for  $T<4.2$  K as shown in Fig. 12(b), but the linear dependence shifts to higher field as  $T$  increases. Since  $k_B T/g\mu_B=1.0$  and 3.1 T at  $T=1.4$  K and 4.2 K, respectively (using the free-electron  $g$  value,  $g=2$ ) this high field behavior is consistent with Eq. (12b). The parameters  $\alpha$  and  $\gamma F_\sigma$  in Eq. (10) can be obtained from the temperature dependence of the conductivity at  $H=0$  and 8 T. At  $H=8$  T, the high-field approximation  $g\mu_B/k_B T=10.8/T \gg 1$  is valid below  $T=4.2$  K, and from Eq. (11) and (12b) we have

$$\begin{aligned} \Delta\sigma_I(H, T) &= \sigma_I(H, 0) + \alpha(4/3 - \gamma F_\sigma/2)T^{1/2} \\ &= \sigma_I(H, 0) + m'T^{1/2}, \end{aligned} \quad (13)$$

where  $\sigma_I(H, 0) = -0.77\alpha(g\mu_B/k_B)^{1/2}\gamma F_\sigma H^{1/2}$ . Using Eqs. (10a) and (13), together with the temperature coefficients  $m$  and  $m'$  ( $H=8$  T) obtained from experiment (see Table II), we find  $\alpha=8/3(3m'-m)$  and  $\gamma F_\sigma=(m'-m)/\alpha$ .

The parameter  $\gamma F_\sigma$  can be alternatively determined from the slope of the high-field dependence in Fig. 12, using Eq. (12b). Figure 13 shows that  $\gamma F_\sigma$  decreases as  $\rho_r$  increases and tends to zero near the transition. Data obtained from both the temperature dependence and the field dependence are consistent, implying that the magnetoconductance at high fields arises mainly from the interaction effects and that localization is less important in strong fields. The free-electron model and the Thomas-Fermi approximation give

$$F = x^{-1} \log_{10}(1+x), \quad (14)$$

where  $x=(2k_F\Lambda_s)^2$  and  $\Lambda_s$  is the Thomas-Fermi screen-

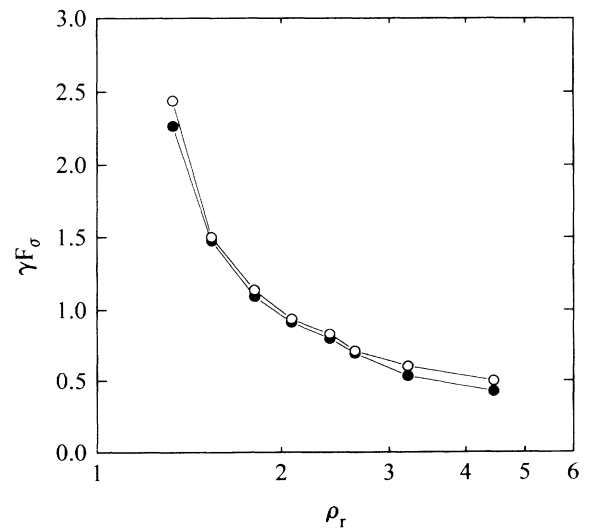


FIG. 13. The interaction parameter,  $\gamma F_\sigma$  calculated from the temperature dependence (●) and high magnetic-field dependence (○) of the conductivity. The data are plotted as a function of  $\rho_r$ .

ing length. Equations (10c) and (14) yield  $0 < F_\sigma < 0.93$  and  $0 < F < 1$ ;  $F \approx 1$  for short-range interactions, and  $F \ll 1$  for long-range interactions.<sup>28</sup> The decrease of  $\gamma F_\sigma$  leads to the change of sign of  $m$  and corresponds to the divergence of screening length near the transition, consistent with McMillan's prediction.<sup>20</sup> Kaveh and Mott<sup>28</sup> argued, however, that inelastic electron-electron scattering dominate. From our value  $0 < \gamma F_\sigma < 2.5$  for  $1 < \rho_r < 5$ , we expect  $\gamma > 2.5$ . For inorganic semiconductors, the "multivalley effect" was introduced to explain the high density of states required for the Hartree term to be large enough to overcome the exchange term in Eq. (10a).<sup>28,35</sup> More detailed theoretical work is required to understand the analogous effect in conducting polymers.

Figure 14 shows the low-field magnetoconductance ( $H < 2$  T) at  $T = 1.4$  K. The magnetoconductance is normalized to  $\alpha\gamma F_\sigma$ . The dashed line in Fig. 14 is the field dependence expected from Eq. (12a) at the same temperature. The data are linear in  $H^2$ , and the slopes at  $\rho_r < 2$  are in good agreement with theory. As  $\rho_r$  increases, however, the slope deviates somewhat from the theoretical value. This can be interpreted as arising from the localization contribution, but the origin of negative magnetoconductance is puzzling. According to the theory of weak localization, the quantum interference between time-reversed backscattering paths is destructive when the spin-orbit scattering is strong, thereby leading to the negative magnetoconductance.<sup>31</sup> This effect has been observed in experiments on disordered metal films<sup>8,36</sup> and in experimental studies of  $p$ -type doped semiconductors.<sup>25</sup> However, on theoretical grounds, one does not expect strong spin-orbit effects in conducting polymers (made up of atoms with relatively low atomic number).

We estimate the contribution of the magnetoconductance at low magnetic fields due to weak (anti-) localization,<sup>31</sup> which can be written as

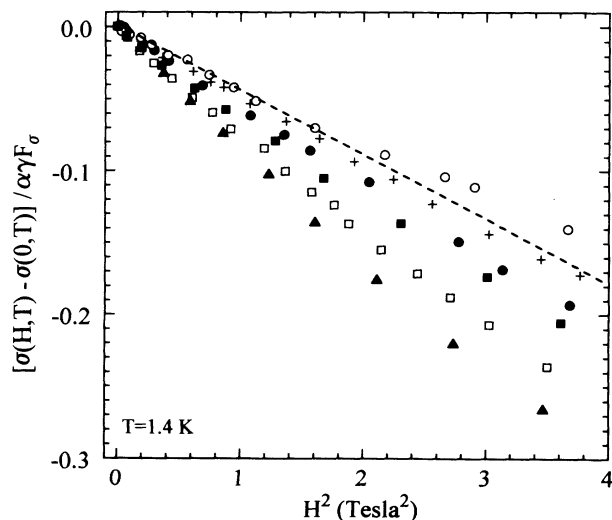


FIG. 14. The low-field magnetoconductance, normalized by  $\alpha\gamma F_\sigma$ , plotted as a function of  $H^2$ : M2 at  $P=9$  kbar ( $\circ$ ),  $\rho_r=1.33$ ), Mc2 at  $P=10$  kbar ( $+$ ,  $\rho_r=1.54$ ), M2 ( $\bullet$ ,  $\rho_r=1.97$ ), Mc2 ( $\blacksquare$ ,  $\rho_r=3.2$ ), Mc3 ( $\square$ ,  $\rho_r=4.5$ ), and Ic1 ( $\blacktriangle$ ,  $\rho_r=12$ ). The dashed line is the theoretical estimate (Ref. 23).

$$\Delta\Sigma_L(H,T) = -(1/48\pi^2)(e/\hbar c)^2 G_0 L_{in}^3 H^2, \quad (15)$$

where  $G_0 = e^2/\hbar$ , and  $L_{in} = (D\tau_{in})^{1/2}$  is the inelastic-scattering length. The interaction and localization contributions are additive. From the deviation in the slopes of the low-field magnetoconductance between experiment and interaction theory, and from Eq. (15), we obtain the inelastic-scattering length as a function of temperature. For samples near the  $M-I$  transition ( $\rho_r > 3$ ), the results are shown in Fig. 15. The temperature dependence of  $L_{in}$  gives  $\tau_{in} \propto L_{in}^2 \propto T^{-p}$  with  $p=1.02 \pm 0.05$ , which is consistent with the theory of the inelastic scattering due to the Coulomb interaction close to the  $M-I$  transition.<sup>26</sup> For samples in the metallic regime ( $\rho_r < 3$ ) the deviation of the slope is small, but we roughly estimate  $L_{in} \sim 200-300$  Å and is nearly temperature independent. In this regime, [from Eq. (10b)]  $D \approx 0.02-0.04$  cm<sup>2</sup>/sec, and the interaction length  $L_T = (\hbar D/k_B T)^{1/2}$  becomes 30-40 Å at  $T=1.4$  K, much lower than the inelastic-scattering length. As the system moves toward the  $M-I$  transition, the disorder increases, the Coulomb interaction is less well screened, thereby decreasing the inelastic electron-electron scattering length. Hence the contribution due to the localization increases with  $\rho_r$ .

#### F. Hopping conduction in the insulating regime

In the insulating (Fermi glass) regime ( $\rho_r > 10$ ), transport occurs through variable-range hopping among localized states as described by Mott (for noninteracting carriers) and by Efros and Shklovskii (when the Coulomb interaction between the electron and the hole left behind is dominant). When the resistivity follows Mott's VRH conduction in three dimensions,<sup>13</sup>

$$\ln\rho(T) \propto (T_{\text{Mott}}/T)^{1/4}, \quad (16a)$$

where  $T_{\text{Mott}} = 18/k_B L_c^3 N(E_F)$ , and  $N(E_F)$  is the density of states at the Fermi level. In the Efros-Shklovskii limit,<sup>14</sup>

$$\ln\rho(T) \propto (T_{\text{ES}}/T)^{1/2}, \quad (16b)$$

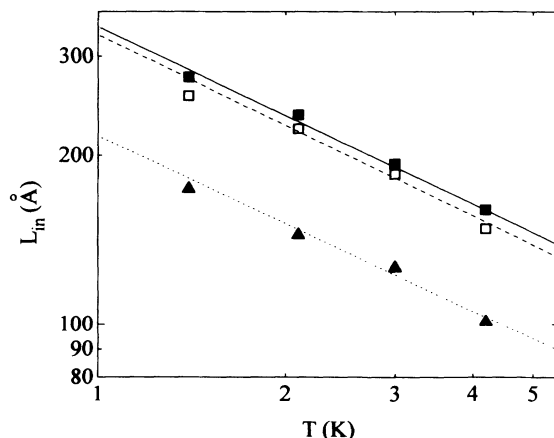


FIG. 15 Log-log plots of the inelastic-scattering length vs  $T$  for samples Mc2 ( $\blacksquare$ ,  $\rho_r=3.2$ ), Mc3 ( $\square$ ,  $\rho_r=4.5$ ), and Ic1 ( $\blacktriangle$ ,  $\rho_r=12$ ).

where  $T_{ES} = \beta_1 e^2 / \epsilon k_B L_c$ ,  $\epsilon$  is the dielectric constant, and  $\beta_1$  is a constant close to 3. A crossover from Mott to Efros-Shklovskii VRH conduction is expected when  $T < T_{ES}$ .

The crossover from Mott to Efros-Shklovskii VRH conduction is observed in the plots of  $\log_{10} W(T)$  vs  $\log_{10} T$  (see the inset of Fig. 2) for samples with  $\rho_r > 100$ . This can be confirmed by the plots of  $\ln \rho(T)$  vs  $T^{-x}$  with  $x = -\frac{1}{4}$  and  $-\frac{1}{2}$  as shown in Fig. 16. Figure 16 shows clearly the linear dependence of  $\log_{10} \rho(T)$  on  $T^{-1/4}$  for samples near the  $M-I$  transition [Fig. 16(a)]. A clear deviation is observed, however, at low temperatures ( $T < 5$  K) for insulating samples [Figs. 16(a) and 16(c)]. For the latter,  $\log_{10} \rho(T)$  is linear in  $T^{-1/2}$  at low temperatures. The characteristic temperature  $T_{Mott}$  and  $T_{ES}$  are determined from the slopes in Figs. 16(a) and 16(b), respectively.

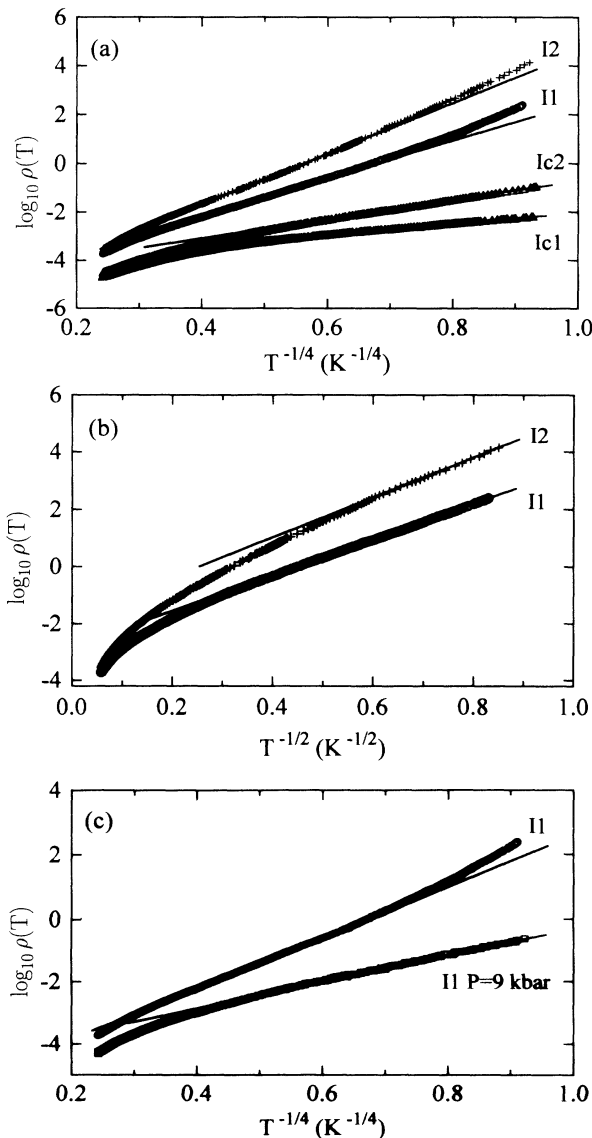


FIG. 16. Temperature dependence of the resistivity for samples in the insulating regime. (a)  $\log_{10} \rho(T)$  vs  $T^{-1/4}$ , (b)  $\log_{10} \rho(T)$  vs  $T^{-1/2}$  for sample I1 and I2, (c)  $\log_{10} \rho(T)$  vs  $T^{-1/4}$  for sample I1 at  $P=9$  kbar and ambient pressure.

ly. For the sample with  $\rho_r = 530$  (sample I1),  $T_{Mott} = 3700$  K and  $T_{ES} = 42$  K, so that  $T_{Mott}/T_{ES} = 88$ . This ratio is in agreement with the theory of Castner,<sup>37</sup> which yields the following expression:

$$T_{Mott}/T_{ES} = 18(4\pi)/\beta_1 = 81 \text{ if } \beta_1 = 2.8. \quad (17a)$$

Using values appropriate for PPy(PF<sub>6</sub>), we estimate  $T_{Mott}/T_{ES} = 81$ . The same theory predicts the crossover temperature  $T_{cross}$  as<sup>37</sup>

$$T_{cross} = 16T_{ES}^2/T_{Mott} = 2.4 \times 10^{-3} T_{Mott} \quad (17b)$$

giving  $T_{cross} = 7.5$  K for the sample with  $\rho_r = 530$  (for  $T_{Mott}/T_{ES} = 88$ ) and  $T_{cross} < 1$  K for samples nearer to the  $M-I$  transition ( $\rho_r < 100$ ), both of which are consistent with experiment.

The Efros-Shklovskii VRH conduction is based on the existence of a Coulomb gap  $\Delta_{CG}$ ,<sup>4</sup>

$$\Delta_{CG} = k_B T_{CG} = e^3 N(E_F)^{1/2} / \epsilon^{3/2}, \quad (18)$$

where  $N(E_F)$  is the unperturbed density of states at the Fermi level (i.e., in the absence of the Coulomb gap) and  $\epsilon = \epsilon_\infty + 4\pi e^2 N(E_F) L_c^2$  with core dielectric constant  $\epsilon_\infty$ . Castner's analysis is valid near the  $M-I$  transition where  $L_c$  is large and  $\epsilon_\infty \ll 4\pi e^2 N(E_F) L_c^2$ . In this limit,

$$\Delta_{CG} = [(4\pi)^{3/2} N(E_F) L_c^3]^{-1} = k_B T_{ES} / \beta_1 (4\pi)^{1/2}, \quad (19)$$

whereas in the opposite limit (far from the  $M-I$  transition where  $L_c$  is small)

$$\Delta_{CG} = e^3 N(E_F)^{1/2} / \epsilon_\infty^{3/2}. \quad (20)$$

For the sample with  $\rho_r = 530$ ,  $T_{CG} = T_{ES}/10$  leading to  $\Delta_{CG} = 0.3$  meV. Near the transition, the localization length increases as  $\rho_r$  decreases, thereby suppressing the Coulomb gap. This suppression was confirmed by the effect of pressure, as shown in Fig. 16(c). The large value of  $T_{Mott}/T_{ES} = 140$  for the sample with  $\rho_r = 2600$  (sample I2) implies that  $4\pi e^2 N(E_F) L_c^2$  approaches  $\epsilon_\infty$  as the localization length decreases.<sup>38</sup>

For samples in the insulating regime, the localization length can be estimated from the expression for the magnetic-field dependence of the Mott VRH resistivity:<sup>14</sup>

$$\log_{10}[\rho(H)/\rho(0)] = t(L_c/L_H)^4 (T_0/T)^{3/4}, \quad (21)$$

where  $t = 5/2016$ , and  $L_H$  is the magnetic length. The plots of  $\log_{10}[\rho(H)/\rho(0)]$  at  $H = 2$  T vs  $T^{-3/4}$  shown in Fig. 17 are consistent with Eq. (21). The deviation at the lowest temperatures for the most insulating sample (I2) corresponds to the crossover to Efros-Shklovskii VRH conduction. From the slopes in Fig. 17, we obtain  $L_c$  (see Table I);  $L_c$  decreases as  $\rho_r$  increases, as expected.

Finally, in Fig. 18, we plot the correlation length  $L_c$  as a function of  $\rho_r$ , in both the insulating regime (the localization length as obtained from Eq. 21) and in the metallic regime [as obtained from  $\sigma(0)$ , using the relation<sup>20</sup>  $\sigma(0) = 0.1e^2/\hbar L_c$ ]. From scaling theory, the correlation length is expected to diverge as the  $M-I$  transition. Since, as shown above, the  $M-I$  transition for PPy(PF<sub>6</sub>) occurs

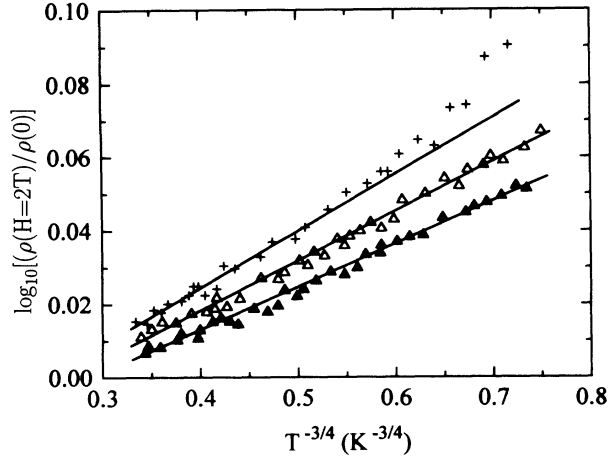


FIG. 17  $\log_{10}[\rho(H)/\rho(0)]$  at  $H=2\text{ T}$  vs  $T^{-3/4}$ ; the localization lengths calculated from the slopes using Eq. (21) are listed in Table I.

at  $\rho_r \sim 10$ , we expect a divergence in  $L_c$  at  $\rho_r \sim 10$ , qualitatively consistent with the data points plotted in Fig. 18.

### G. Thermoelectric power

Figure 19 shows the temperature dependence of thermoelectric power  $S(T)$  for PPy(PF<sub>6</sub>). At room temperature,  $S_{RT} = +7.5$  to  $+12\ \mu\text{V/K}$ , decreasing somewhat as  $\rho_r$  decreases. The magnitude and the sign of  $S(T)$  are similar to results obtained from other  $p$ -type doped conducting polymers.<sup>10,11</sup> The linear temperature dependence of  $S(T)$  corresponds to the characteristic diffusion thermopower of a metal. No phonon drag contribution was observed, consistent with expectations, since the phonon drag contribution is suppressed by disorder.<sup>39</sup>

For a disordered system with a partially filled band, there is a finite density of states at the Fermi energy. When  $E_F$  lies in the regime of extended states, the system is a metal for which  $S(T)$  can be expressed as

$$S(T) = (\pi^2/3)(k_B/e)(k_B T)[d \log_{10} \sigma(E)/dE]_{E_F}, \quad (22)$$

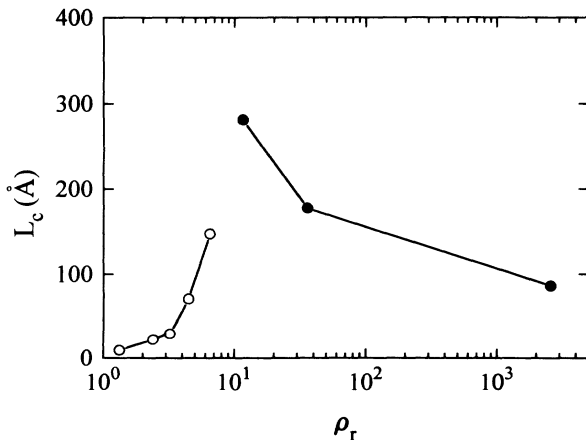


FIG. 18. The correlation length ( $L_c$ ) obtained from the insulating (●) and the metallic (○) regimes plotted as a function of  $\rho_r$ , see text.

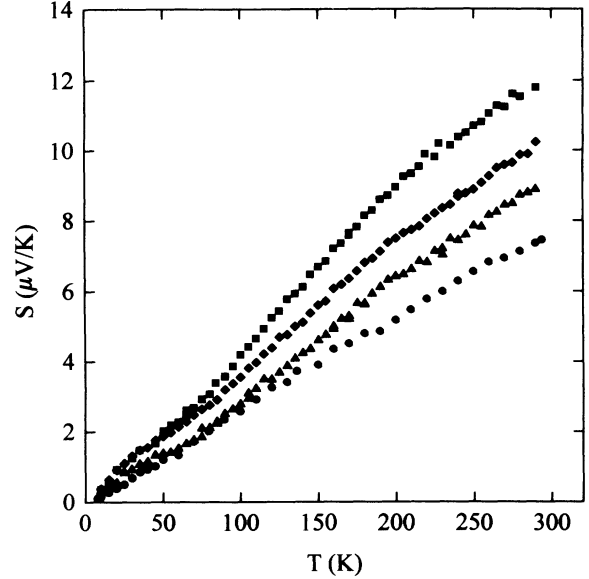


FIG. 19. Temperature dependence of thermoelectric power  $S(T)$  for samples I2 (■), Ic1 (◆), Mc1 (▲), and M1 (●).

where the energy dependence of  $\sigma(E)$  arises from a combination of the band structure and the energy dependence of the mean scattering time  $\tau(E)$ . If we assume that  $\sigma(E)$  is a slowly varying function in the vicinity of  $E_F$ , Eq. (20) is equivalent to the free-electron approximation result,

$$S(T) = +(\pi^2/3)(k_B/|e|)(k_B T)(z/E_F), \quad (23)$$

where the positive sign indicates that the partially filled  $\pi$  band is holelike, and  $z$  is a constant determined from the band structure and  $\tau(E)$ . The density of states at Fermi level  $N(E_F)$  estimated from Eq. (23)<sup>40</sup> is  $N(E_F) \approx 1.0$ – $1.6$  states per eV per 4 pyrrole units (assuming that ideal doping level is reached; i.e., approximately one dopant per four pyrrole units). The relatively large magnitude of  $S(T)$  in comparison with typical metals suggests that the partially filled  $\pi$  band is relatively narrow,  $< 1\text{ eV}$ .

The theory of hopping thermopower, expected to be valid in the insulating regime, predicts  $S(T) \propto T^{1/2}$  for Mott VRH in  $3d$  and  $S(T) = \text{constant}$  for Efros-Shklovskii VRH conduction.<sup>39</sup> Both are inconsistent with the data in Fig. 19. Although this is not understood, the extension of the linear dependence of  $S(T)$  into the insulating regime appears to be a general feature of conducting polymers near the  $M$ - $I$  transition.<sup>10,11</sup> This discrepancy might originate from the anisotropy associated with the quasi-one-dimensional electronic structure; a feature not included in the standard theories. Qualitatively, the linear temperature dependence of  $S(T)$  in insulating samples suggests that the quasi-one-dimensional electronic structure of the PPy chains is very close to that of a metal.

### IV. SUMMARY AND CONCLUSION

We have investigated the transport properties of heavily doped PPy(PF<sub>6</sub>) as a function of the disorder as characterized by the resistivity ratio,  $\rho_r = \rho(1.4\text{ K})/\rho(300$

K). As the disorder is reduced,  $\rho_r$  systematically decreases. Heavily doped PPy(PF<sub>6</sub>) passes through the transition from insulator to metal near  $\rho_r \approx 10$ . Application of high pressure decreases  $\rho_r$ , and enables fine tuning of the metal-insulator transition.

As heavily doped PPy(PF<sub>6</sub>) approaches the  $M$ - $I$  transition from the metallic regime ( $\rho_r \sim 1-6$ ), (i)  $\sigma(0)$  decreases continuously, and the correlation length correspondingly increases. The thermopower is positive and linear in  $T$  with magnitude consistent with metallic transport; (ii) the screening length increases,  $\gamma F_\sigma$  decreases, and the effect of the electron-electron interaction on the resistivity increases; (iii) the sign of temperature coefficient of  $\rho(T)$  changes, at low temperatures, from positive to negative at  $\rho_r \approx 2$ ; (iv) when  $\rho_r < 2$ , the temperature  $T_m$  of the conductivity minimum decreases with increasing  $\rho_r$ , and the inelastic-scattering mechanism at  $T > T_m$  is due to the electron-phonon interaction ( $p=2.5$ ); (v) near the  $M$ - $I$  transition, the inelastic-diffusion length decreases, and the contribution due to the localization increases. In the critical regime of the metal-insulator transition, the resistivity exhibits a power-law temperature dependence (in agreement with theory), and the power-law exponent  $\beta$  decreases from 0.3 to 1 as  $\rho_r$  increases.

As the heavily doped PPy(PF<sub>6</sub>) passes from  $M$ - $I$  tran-

sition into the insulating regime ( $\rho_r > 10$ ), (i) the localization length decreases as  $\rho_r$  increases; (ii) a Coulomb gap opens, and the magnitude of the Coulomb gap increases as  $\rho_r$  increases; (iii) the magnitude of the thermoelectric power increases, but the temperature dependence remains linear, implying that the quasi-one-dimensional structure of PPy is very close to that of a metal.

The correlation length is shown to increase as the disorder, characterized by  $\rho_r$ , approaches the  $M$ - $I$  transition from either side. Since the  $M$ - $I$  transition for PPy(PF<sub>6</sub>) occurs at  $\rho_r \sim 10$ , we expect a divergence in  $L_c$  at  $\rho_r \sim 10$ , qualitatively consistent with the values for  $L_c$  inferred from the extrapolated  $\sigma(0)$  in the metallic regime and from analysis of the VRH magnetoresistance in the insulating regime. Thus, by using  $\rho_r$  to characterize the magnitude of the disorder, we have developed a complete and fully consistent picture of the  $M$ - $I$  transition in PPy(PF<sub>6</sub>).

#### ACKNOWLEDGMENTS

This work was partially supported by the MRL program of the National Science Foundation under Award No. DMR-9123048, and partially supported by a research grant from the Electric Power Research Institute (EPRI). C.O.Y. was supported in part by the Korean Science and Engineering Foundation (KOSEF).

- <sup>1</sup>M. Yamamura, T. Hagiwara, and K. Iwata, *Synth. Met.* **26**, 209 (1988).
- <sup>2</sup>K. Sato, M. Yamamura, T. Hagiwara, K. Murata, and M. Tokumoto, *Synth. Met.* **40**, 35 (1991).
- <sup>3</sup>T. Ishiguro, H. Kaneko, T. Nogami, H. Ishimoto, H. Nishiyama, J. Tsukamoto, A. Takahashi, M. Yamaura, T. Hagiwara, and K. Sato, *Phys. Rev. Lett.* **69**, 660 (1992).
- <sup>4</sup>V. V. Bryskin, *Fiz. Tverd. Tela (Leningrad)* **28**, 2981 (1986) [*Sov. Phys. Solid State* **28**, 1676 (1986)].
- <sup>5</sup>M. Reghu, C. O. Yoon, D. Moses, and A. J. Heeger, *Synth. Met.* (to be published).
- <sup>6</sup>Y. W. Park, C. Park, Y. S. Lee, C. O. Yoon, H. Shirakawa, Y. Suezaki, and K. Akagi, *Solid State Commun.* **65**, 147 (1988).
- <sup>7</sup>J. Tsukamoto, *Adv. Phys.* **41**, 509 (1992), and references therein.
- <sup>8</sup>Reghu M., Y. Cao, D. Moses, and A. J. Heeger, *Phys. Rev. B* **47**, 1758 (1993); Reghu M., C. O. Yoon, Y. Cao, D. Moses, and A. J. Heeger, *ibid.* **48**, 12 685 (1993).
- <sup>9</sup>N. S. Sariciftci, Y. Cao, and A. J. Heeger, *Phys. Rev. B* (to be published).
- <sup>10</sup>A. B. Kaiser, *Phys. Rev. B* **40**, 2806 (1989).
- <sup>11</sup>C. O. Yoon, Reghu M., Y. Cao, D. Moses, and A. J. Heeger, *Phys. Rev. B* **48**, 14 080 (1993).
- <sup>12</sup>K. Lee, A. J. Heeger, and Y. Cao, *Phys. Rev. B* **48**, 14 884 (1993).
- <sup>13</sup>N. F. Mott and E. A. David, *Electronic Processes in Noncrystalline Materials* (Oxford University Press, Oxford, 1979); N. F. Mott, *Metal-Insulator Transition*, 2nd ed. (Taylor & Francis, London, 1990).
- <sup>14</sup>B. I. Shklovskii and A. L. Efros, *Electronic Properties of Doped Semiconductors* (Springer-Verlag, Berlin, 1979).
- <sup>15</sup>H. Fujiwara, H. Kadomatsu, and K. Tohma, *Rev. Sci. Instrum.* **51**, 1345 (1980).
- <sup>16</sup>Y. W. Park, *Synth. Met.* **45**, 173 (1991).
- <sup>17</sup>R. B. Roberts, *Philos. Mag.* **36**, 91 (1977).
- <sup>18</sup>A. G. Zabrodskii and K. N. Zinov'eva, *Zh. Eksp. Teor. Fiz.* **86**, 727 (1984) [*Sov. Phys. JETP* **59**, 345 (1984)].
- <sup>19</sup>E. Abrahams, P. W. Anderson, D. C. Liccardello, and T. V. Ramakrishnan, *Phys. Rev. Lett.* **42**, 673 (1979).
- <sup>20</sup>W. L. McMillan, *Phys. Rev. B* **24**, 2739 (1981).
- <sup>21</sup>A. I. Larkin and D. E. Khmel'nitskii, *Zh. Eksp. Teor. Fiz.* **83**, 1140 (1982) [*Sov. Phys. JETP* **56**, 647 (1982)].
- <sup>22</sup>B. L. Altshuler and A. G. Aronov, *Zh. Eksp. Teor. Fiz.* **77**, 2028 (1979) [*Sov. Phys. JETP* **50**, 968 (1979)]; *Pis'ma Zh. Eksp. Teor. Fiz.* **30**, 514 (1979) [*JETP Lett.* **30**, 482 (1979)].
- <sup>23</sup>P. A. Lee and T. V. Ramakrishnan, *Rev. Mod. Phys.* **57**, 287 (1985).
- <sup>24</sup>N. F. Mott and M. Kaveh, *Adv. Phys.* **34**, 329 (1985).
- <sup>25</sup>P. Dai, Y. Zhang, and M. P. Sarachik, *Phys. Rev. B* **45**, 3984 (1992); P. Dai, Y. Zhang, and M. P. Sarachik, *ibid.* **46**, 6724 (1992).
- <sup>26</sup>D. Beliz and K. I. Wysokinski, *Phys. Rev. B* **36**, 9333 (1987).
- <sup>27</sup>Y. Imry, *J. Appl. Phys.* **52**, 1817 (1981).
- <sup>28</sup>M. Kaveh and N. F. Mott, *Philos. Mag.* **B 55**, 1 (1987).
- <sup>29</sup>T. F. Rosenbaum, R. F. Milligan, M. A. Paalanen, G. A. Thomas, R. N. Bhatt, and W. Lin, *Phys. Rev. B* **27**, 7509 (1983).
- <sup>30</sup>B. I. Shklovskii and B. Z. Spivak, in *Hopping Transport in Solids*, edited by M. Pollak and B. I. Shklovskii (Elsevier/North-Holland, Amsterdam, 1990).
- <sup>31</sup>A. Kawabata, *Solid State Commun.* **34**, 431 (1980); B. L. Altshuler and A. G. Aronov, in *Electron-Electron Interactions in Disordered Systems*, edited by A. L. Efros and M. Pollak

- (North-Holland, Amsterdam, 1985).
- <sup>32</sup>Reghu M., K. Vakiparta, Y. Cao, and D. Moses (unpublished); Reghu M., K. Vakiparta, C. O. Yoon, Y. Cao, D. Moses and A. J. Heeger, *Synth. Met.* (to be published).
- <sup>33</sup>Assuming ideal doping, with four pyrrol-PF<sub>6</sub> units per repeat unit and a density for doped PPy of  $d=1.3$ ,  $n=1.9 \times 10^{21}$  cm<sup>-3</sup>.
- <sup>34</sup>D. E. Khmel'niskii and A. I. Larkin, *Solid State Commun.* **39**, 1069 (1981).
- <sup>35</sup>R. N. Bhatt and P. A. Lee, *Solid State Commun.* **48**, 755 (1983).
- <sup>36</sup>G. Bergman, *Phys. Rev. B* **28**, 2914 (1983).
- <sup>37</sup>T. G. Castner, in *Hopping Transport in Solids* (Ref. 30).
- <sup>38</sup>R. Rosenbaum, *Phys. Rev. B* **44**, 3599 (1991).
- <sup>39</sup>I. P. Zvyagin, *Phys. Status Solidi B* **58**, 443 (1973); in *Hopping Transport in Solids* (Ref. 30).
- <sup>40</sup>Y. W. Park, A. J. Heeger, M. A. Drury, and A. G. MacDiarmid, *J. Chem. Phys.* **73**, 94 (1980).